

## Research Article

# Design Analysis and Test Verification of Double-Layer Gradient Coating Reinforced Concrete Flexural Strength

Qiang Pei <sup>1</sup>, Yihan Xiang,<sup>1</sup> Shuncai Hu,<sup>1</sup> Yiwang Bao,<sup>2</sup> and Weihong Li <sup>1</sup>

<sup>1</sup>Dalian University, College of Architectural Engineering, Dalian 116622, China

<sup>2</sup>China Academy of Building Materials Science, Beijing 100024, China

Correspondence should be addressed to Weihong Li; [liweihong@dlu.edu.cn](mailto:liweihong@dlu.edu.cn)

Received 22 February 2022; Revised 11 April 2022; Accepted 28 April 2022; Published 6 June 2022

Academic Editor: Awais Ahmed

Copyright © 2022 Qiang Pei et al. This is an open access article distributed under the Creative Commons Attribution License, which permits unrestricted use, distribution, and reproduction in any medium, provided the original work is properly cited.

The residual compressive stress of concrete members can offset the tensile stress caused by some external load and hinder the generation and expansion of surface cracks to enhance the flexural strength of concrete. In order to carry out this strengthening method, the single-layer and double-layer gradient coatings mixed by sulphate aluminium cement with different amounts of expansion agent on the surface of concrete specimens were discussed, and the theoretical calculation formula of surface compressive stress caused by this was deduced. Combined with experimental data, the influence of surface compressive stress on flexural strength of concrete was studied. The results demonstrate that the greater the surface compressive stress generated in the coating, the better the effect of improving the flexural strength of concrete. To obtain sufficient surface compressive stress, it is recommended that the cross-sectional product ratio of the substrate to the coating is more than 80; the higher the elastic modulus of the coating, the greater the surface compressive stress; the smaller the shrinkage rate of the coating, the greater the surface compressive stress. The improvement effect of double-layer gradient coating on the flexural strength of concrete is better than that of single-layer coating. Compared with the reference specimen without coating, the improvement rates of double-layer gradient coating on the early and late flexural strength of concrete are 57.7% and 45.7%, respectively.

## 1. Introduction

Concrete has become the most widely used civil engineering materials in practical construction projects due to its high compressive strength, low cost, easy access to raw materials, and convenient construction. It plays a key role in promoting the development of social economy. With the development of science and technology, concrete buildings will gradually develop in the direction of large scale, high layers and large span in the future. However, the low flexural strength of most concrete used nowadays can lead to surface cracking of large concrete structures (such as foundation slab, wall slab, floor slab and underground structure, etc.), and even affect the safety performance and service life of concrete structures. [1–3]. Improving the flexural strength of concrete through diverse ways has become one of the

urgent problems to be solved, so it has gradually become a research hotspot of experts and scholars.

The incorporation of reinforcement with high tensile strength in concrete is one of the first measures to enhance the flexural strength of concrete structures, and the premature cracking of concrete in the tensile area limited the use of reinforced concrete components in large span or bearing power load structures. The emergence of prestressed concrete solves this problem. It uses the high compressive strength of concrete to make up for its low flexural strength and utilizes the precompression method to indirectly improve the flexural strength of concrete. In essence, it changes the crack-prone characteristics of concrete, which is very effective for saving steel, reducing the size of the structural section, reducing the weight of the structure, preventing cracking, and reducing deflection. In addition, with

the further development of research and development work, various mineral admixtures, fibers, additives, and nanophase materials, polymer has been applied by scholars to improve the flexural strength of concrete and has achieved good results. The research status is as follows:

Tolmachov et al. [4] added water reducer, mineral admixture, and fiber into concrete to increase its flexural strength by 25.7%. Singh et al. [5] found that the flexural strength of RAP concrete could be increased by 10% by adding 10% (mass fraction) silica fume. Zhang et al. [6] found that when the fly ash content was 20% (mass fraction, the same below), the flexural strength of recycled concrete could be increased by 29.9%. On this basis, the flexural strength could be further increased by 11.4% by adding 1% water reducer, while the flexural strength of concrete could be increased by 30.7% by adding 10% silica fume. Somasekharaiah [7] showed that when 10% silica fume was added to the concrete, and 1% steel fiber and 0.25% polypropylene fiber were mixed in the concrete, the strength improvement rate reached 71.5%. Mahadik et al. [8] found that different dosages (volume fraction of 0.25%~1%) of steel fiber had different degrees of improvement effect on the flexural strength of concrete, and when the dosage was 0.75%, it was the best, and the improvement rate reached 43.3%. Bhat and Alam [9] found through a large number of tests in the concrete mixed with 0.5% to 2% (volume fraction) of steel fibers can improve its flexural strength, the flexural strength of concrete at the early age became the highest when the steel fiber content was 2%. Bi et al. [10] found that the flexural strength of polypropylene fiber with a length of 18 mm and a dosage of  $0.6 \text{ kg/m}^3$  was increased by 32.3% when it was mixed with concrete.

Turlapati and Chintapalli [11] suggested that the flexural strength of polypropylene fiber with a volume fraction of 1% could be increased by 35%. Wyrzykowski et al. [12] combined expansion agent, super absorbent polymer, and shrinkage-reducing agent to make the prestress of central concrete reach about 2.5 MPa~3.0 MPa. Yang et al. [13] found that when the content of expansive agent was 6% (mass fraction), the early and late flexural strength of concrete could be enhanced by 6.2% and 4.1%, respectively. Li et al. [14] found that when the content of nanosilica was 5% (mass fraction), the flexural strength of lightweight concrete could be enhanced by 17.5%. Saafi et al. [15] incorporated 0.35% reduced graphite oxide into cement-based composites, resulting in an increase of 134% in flexural strength. Wang et al. [16] found that the flexural strength of concrete could be increased by 12% by adding 0.5% carbon nanotubes and 1.0% polyvinyl alcohol nanosecond emulsion. Liu et al. [17] added 7% acrylic acid (AA) and 1-acrylamido-2-methylpropanesulfonic acid (AMPS) polymer into concrete to increase its flexural strength by 61.2%.

However, all of the above technical ways to improve the flexural strength of concrete have limitations. The production process of prestressed concrete members is complex, the technical requirements are high, and special tension equipment and professional technical operators are needed. At the same time, the construction cost of prestressed concrete structures is large, and the engineering cost of fewer

components is high. The application of mineral admixtures in concrete provides a driving force for the sustainable development of resources, and its beneficial effect on the performance of concrete is no doubt. However, industrial waste residue used as mineral admixtures is after all an industrial byproduct, so there are also some problems. For example, silica fume will aggravate the shrinkage of concrete, and fly ash and slag will reduce the initial mechanical properties of concrete. At the same time, the measures taken to stimulate the activity of mineral admixtures may lead to hidden dangers such as alkali aggregate reaction, weak resistance to sulfate attack, and poor compatibility of admixtures [18–22]. The incorporation of fiber into concrete can significantly enhance the flexural strength of concrete, while studies have shown that the incorporation of steel fiber has no obvious enhancement effect on the compressive strength of concrete, and there are also problems such as high unilateral cost and construction difficulties. Basalt fiber production process energy consumption is enormous, and process control is not easy. Ordinary glass fiber is brittle and easy to break, easy to be damaged in the mixing process, and plant fibers have problems such as elevated water absorption, poor alkali resistance, and difficult processing [23, 24]. Nanomaterials are not only expensive but also need to consider the dispersion problem in the use process, and their application in concrete needs to be further studied [25, 26]. There continue to be some deficiencies in the overall performance of polymer concrete when it is modified by a single polymer. The incorporation of chemical admixtures will lead to changes in the structural quality of polymer membranes, which will have a negative impact on concrete [27, 28].

In addition to the abovementioned prestressed concrete, another successful application of prestressed reinforcement technology is the tempered glass. The tempered glass can improve the strength of the glass by 2~5 times by forming a layer of preloading stress on the surface of the ordinary glass, and at the same time, it can improve its thermal stability and safety performance, and it has been comprehensively promoted and popularized worldwide since the beginning of the 20th century [29–31]. Both in the field of concrete and glass, prestressed reinforcement design of macroscopic structure is adopted. The compressive stress is introduced into the material or component in advance to offset the external tensile stress, so as to increase the strain of the matrix cracking due to tension, and improve the fracture strength, reliability, and durability of the material. In recent years, a prestress design of high strength and high damage tolerance composite ceramics comparable to the prestress distribution of tempered glass has produced good results [32, 33]. In fact, as long as it can be realized, this method can be applied to any brittle material, and concrete is one of the typical brittle materials, with the property of compressive and tensile resistance. Therefore, this study introduces the idea of surface prestress design into concrete. By double-layer gradient coating of sulphate aluminium cement with different expansion agents, Because of the difference shrinkage rate between Coating 1 and Coating 2, Coating 1 and concrete, the surface residual compressive stress is formed on concrete surface to offset the flexural stress

caused by external load, so as to prevent or reduce the formation and expansion of surface cracks, thereby improving the flexural strength of concrete and extending its service life. The method is simple to operate, not limited by the component size and shape, and more economical, while the substrate does not need to consider the compatibility with the new material, which has good application prospects.

## 2. Theoretical Analysis

The principle of prestressed concrete to enhance the flexural strength of structural members is to produce precompression stress in concrete and pretension stress in steel through the reinforcement in the tensile zone. The precompression stress can reduce or offset the tensile stress caused by the external load, so that the tensile stress of structural members is not large or even in the compression state, so as to improve the flexural strength of concrete structural members. In turn, coating the surface of the tensile zone of concrete with coating shrinkage rate less than the shrinkage rate of the substrate will produce precompression stress on the surface of the concrete and produce a balanced pretension stress inside the concrete, which is the same as the principle of improving the flexural strength of prestressed concrete. Only one of the precompression stresses is generated inside the concrete, and one is generated on the surface of the concrete. If a double-layer gradient coating with different shrinkage rates is applied on the concrete surface, the second coating (coating 2) shrinkage rate < the first coating (coating 1) shrinkage rate, the surface residual compressive stress in both coating 1 and coating 2, the double-layer gradient coating, which can further enhance the flexural strength of the concrete. The residual stress distribution diagram of prestressed concrete, single-layer coated concrete, and double-layer gradient-coated concrete is shown in Figure 1.

To determine the feasibility of this idea, this paper first derived the theoretical calculation formula of the surface compressive stress generated by applying double-layer gradient coating, assuming the contraction ratio of coating 1 and coating 2 is  $\alpha_{c1}$  with  $\alpha_{c2}$ , and the shrinkage rate of concrete substrate is  $\alpha_s$ , the cross-sectional diagram of the length direction of the test piece before and after the coating is shown in Figure 2. Assuming that no constraint exists in the ideal free shrinkage case, the shrinkage of coating and substrate is shown in the dashed line section of Figure 2, and the shrinkage rate of coating 1, coating 2, and substrate can be indicated by formula (1), (2) and (3).

$$\alpha_{c1} = \frac{\delta_{11}}{L}, \quad (1)$$

$$\alpha_{c2} = \frac{\delta_{12}}{L}, \quad (2)$$

$$\alpha_s = \frac{\delta_2}{L}. \quad (3)$$

In the formula, the amount of free contraction of the coating 1 and the coating 2 is  $\delta_{11}$  and  $\delta_{12}$ ,  $\delta_2$  is the length direction

of the substrate, and  $L$  is the initial length of the sample. In fact, because the tight binding of the interface has deformed the coating identical to the substrate, assuming that the overall amount of cooperative deformation of the composite sample is  $\bar{\alpha}$ , and the overall shrinkage rate is  $\bar{\alpha}$ :

$$\bar{\alpha} = \frac{\delta}{L}. \quad (4)$$

The residual stress in the coating and the substrate is balanced, assuming the surface compressive stress in the coating 1 and the coating 2 are  $\sigma_{c1}$  and  $\sigma_{c2}$ , the tensile stress in the substrate to balance the surface compressive stress is  $\sigma_s$ , under the action of stress, the linear deformations of coating 1 and coating 2 are  $d_{11}$  and  $d_{12}$ , the linear deformation of the substrate is  $d_2$ . According to the relationship between stress and strain, formulas (5), (6), and (7) can be obtained:

$$d_{11} = \frac{\sigma_{c1}}{E_{c1}} \times L. \quad (5)$$

$$d_{12} = \frac{\sigma_{c2}}{E_{c2}} \times L. \quad (6)$$

$$d_2 = \frac{\sigma_s}{E_s} \times L. \quad (7)$$

The elastic modulus of the coating 1 and the coating 2 is  $E_{c1}$  and  $E_{c2}$ , respectively,  $E_s$  is the elastic modulus of the substrate, which is known or tested. To facilitate derivation and analysis, assuming the cross-section area of the coating 1 and the coating 2 is equal, known from the substrate tensile stress and the coating compressive stress in the cross section:

$$\sigma_{c1}S_c + \sigma_{c2}S_c = -\sigma_sS_s. \quad (8)$$

From Figure 2,  $d_{11}$ ,  $d_{12}$ ,  $\delta_{11}$ ,  $\delta_{12}$ , and  $\delta_2$  has the following geometric relationship:

$$d_{11} = \delta - \delta_{11}, \quad (9)$$

$$d_{12} = \delta - \delta_{12}, \quad (10)$$

$$d_2 = \delta_2 - \delta. \quad (11)$$

Combined with formula (3), (4), (7), (8) and (11) can get formula (12):

$$\sigma_{c1} + \sigma_{c2} = \left( \frac{S_s}{S_c} \right) \cdot E_s \cdot (\alpha_s - \bar{\alpha}). \quad (12)$$

It can be seen by formula (12) that the surface compressive stress is not a material constant, and it is related to the cross-sectional product ratio of the coating to the substrate. In order to more intuitively evaluate the surface compressive stress of various shapes and dimensions, it is best to use the material constant instead of the unknown quantity, and the extraordinary parameters can be expressed in combination with the

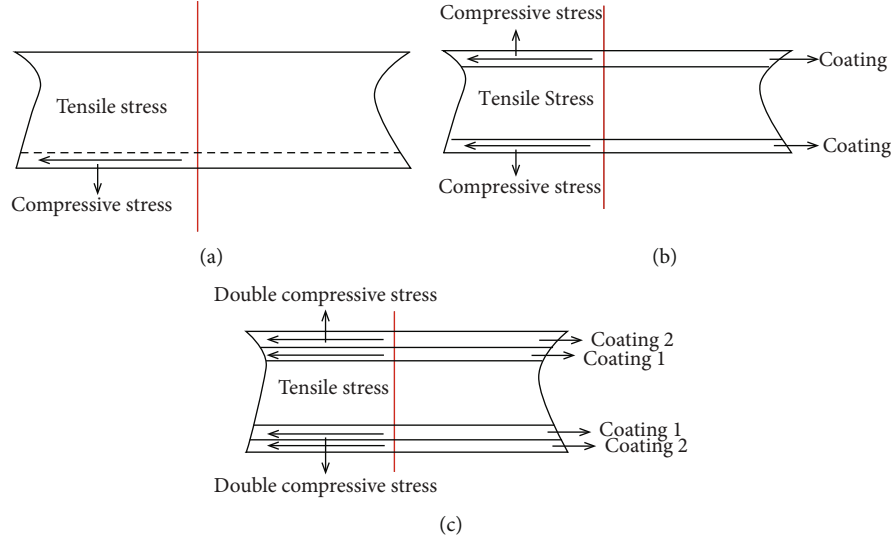


FIGURE 1: Residual stress distribution diagram of prestressed concrete (a), single-layer coating concrete (b), and double-layer gradient coating concrete (c).

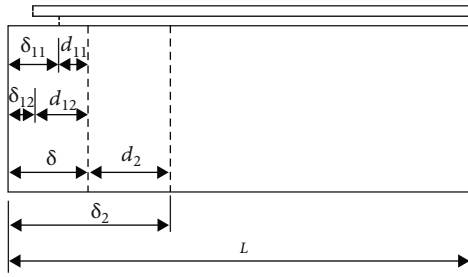


FIGURE 2: Cross-sectional diagram of coating specimen.

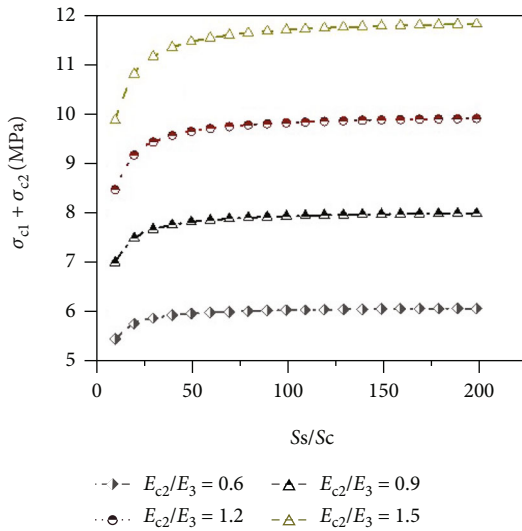


FIGURE 3: Theoretical relationship between surface compressive stress and cross-sectional area ratio under four modulus ratios.

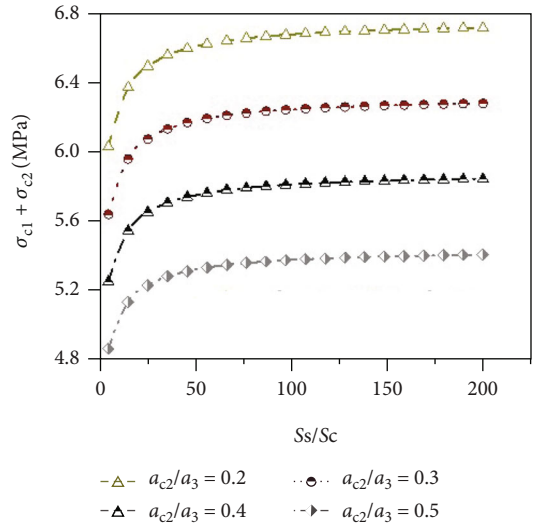


FIGURE 4: Theoretical relationship between surface compressive stress and cross-sectional area ratio under four shrinkage ratios.

TABLE 1: Chemical composition of cement and expansion.

Material	CaO	SiO <sub>2</sub>	Al <sub>2</sub> O <sub>3</sub>	SO <sub>3</sub>	Fe <sub>2</sub> O <sub>3</sub>	MgO
P·O42.5R	56.78	22.61	7.01	1.94	2.89	3.73
SAC42.5	49.50	8.51	20.17	14.91	1.97	0.77
HME®-IV	52.56	1.03	13.61	28.33	0.66	1.81

above formula:

$$\bar{\alpha} = \frac{[E_{c1}\alpha_{c1} + E_{c2}\alpha_{c2} + E_s \cdot \alpha_s \cdot (S_s/S_c)]}{[E_{c1} + E_{c2} + E_s \cdot (S_s/S_c)]}. \quad (13)$$

Combining equation (12) and equation (13), the calculation formula of surface compressive stress caused by double-

TABLE 2: Performance indicators of the expansion agent.

Inspection item	Fineness		Limited expansion Rate (%)		Compressive strength (MPa)	
	Sieve residue (1.18 mm) (%)	Specific surface area (m <sup>2</sup> ·kg <sup>-1</sup> )	In water (7d)	In air (21d)	7d	28d
Performance indicator	0	390	0.102	0.034	40.0	53.4

TABLE 3: Mixture ratio of coating and substrate.

Sample no.	Mixture ratio of substrate (kg·m <sup>-3</sup> )				Mixture ratio of coating (%)	
	C	W	S	G	SAC42.5	HME®-IV
Control	350	190	648	1177	/	/
SC -0%	350	190	648	1177	100%	0%
SC -6%	350	190	648	1177	94%	6%
SC -10%	350	190	648	1177	90%	10%
DC-0%-10%	350	190	648	1177	Coating 1: 100% Coating 2: 90%	Coating 1: 0% Coating 2: 10%

layer gradient coating can be obtained:

$$\sigma_{c1} + \sigma_{c2} = \left( \frac{S_s}{S_c} \right) \cdot E_s \cdot \alpha_s \left\{ 1 - \left[ \frac{E_{c1}\alpha_{c1}}{E_s\alpha_s} + \frac{E_{c2}\alpha_{c2}}{E_s\alpha_s} + \frac{S_s}{S_c} \right] / \left[ \frac{E_{c1}}{E_s} + \frac{E_{c2}}{E_s} + \frac{S_s}{S_c} \right] \right\}. \quad (14)$$

Similarly, the formula for the surface compressive stress generated by a single-layer coating can be deduced as described above:

$$\sigma_c = \left( \frac{S_s}{S_c} \right) \cdot \left\{ 1 - \left[ \frac{E_s S_s}{E_c S_c} + \frac{\alpha_c}{\alpha_s} \right] / \left[ 1 + \frac{E_s S_s}{E_c S_c} \right] \right\} E_s \cdot \alpha_s. \quad (15)$$

In the formula,  $\sigma_s$  is the tensile stress generated in the substrate and balanced with the surface compressive stress,  $S_c$  and  $S_s$  are the cross-sectional areas of coating and substrate, respectively.  $E_c$  and  $E_s$  are the elastic modulus of coating and substrate, respectively,  $\alpha_c$  and  $\alpha_s$  are the shrinkage of coating and substrate, respectively.

It can be seen from formula (14) that the magnitude of the surface compressive stress in the double-layer gradient coating is closely related to the cross-sectional area ratio, elastic modulus ratio and shrinkage ratio between the coating and the substrate. Therefore, the magnitude of surface compressive stress can be adjusted by these parameters to achieve the effect of optimal design. In this paper, the cross-sectional product of the concrete substrate has been determined, and its shrinkage rate and elastic modulus are also a fixed value (Obtained  $\alpha_s = 330 \times 10^{-6}$ ,  $E_s = 28.1$  GPa through test), allowing qualitative analysis of surface compressive stress generated in double-layer gradient coating based on formula (14).

First, the elastic modulus value and contraction rate value of coating 1 are taken as the invariants, and when the shrinkage and elastic modulus of coating 2 are variables,

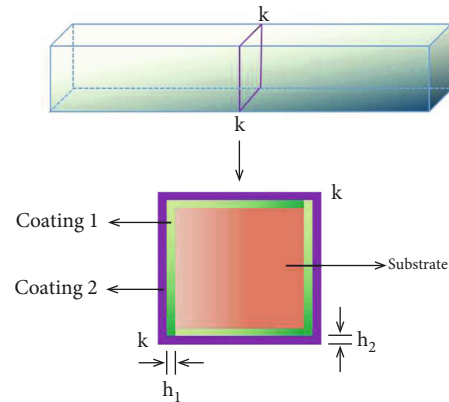


FIGURE 5: Schematic of the double-coated specimen.

the variation trend of the surface compressive stress generated in the double-layer gradient coating with the ratio of the cross-sectional area of the substrate to the coating is analyzed. It is assumed that the shrinkage ratios of coating 1 and coating 2 to substrate ( $\alpha_{c1}/\alpha_s = 0.6$ ,  $\alpha_{c2}/\alpha_s = 0.3$ ) are both fixed values. When the elastic modulus ratio of coating 1 to substrate is  $E_{c1}/E_s = 0.6$ , and the elastic modulus ratio of coating 2 to substrate is  $E_{c2}/E_s = 0.6 \times 0.9 \times 1.2 \times 1.5$ , respectively, the variation trend of surface compressive stress in the double-layer gradient coating with the cross-sectional area ratio of substrate to coating is shown in Figure 3. It is assumed that the elastic modulus ratio of coating 1 and coating 2 to substrate ( $E_{c1}/E_s = 0.8$ ,  $E_{c2}/E_s = 0.5$ ) is a fixed value. When the shrinkage ratio of coating 1 to substrate is  $\alpha_{c1}/\alpha_s = 0.6$ , and the shrinkage ratio of coating 2 to substrate is  $\alpha_{c2}/\alpha_s = 0.2, 0.3, 0.4, 0.5$ , respectively, the variation trend of the surface compressive stress generated in the double-layer gradient coating with the cross-sectional area ratio of the substrate to the coating is shown in Figure 4.



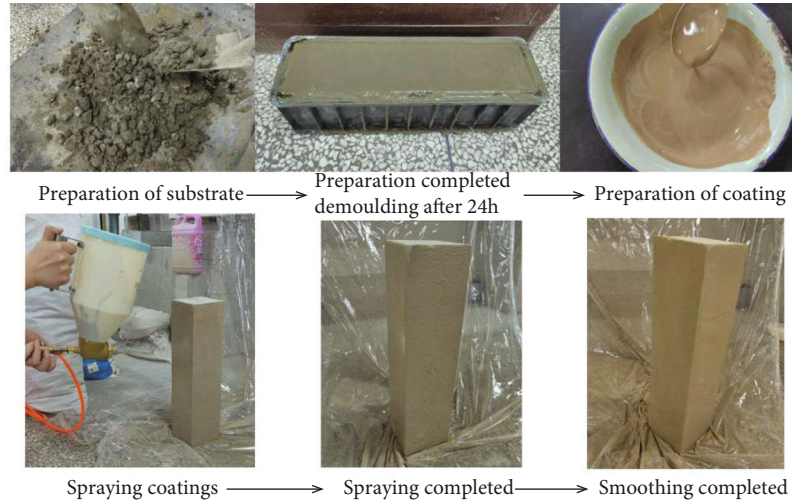


FIGURE 6: Preparation process of coated concrete specimen.

As shown from Figure 3, when the elastic modulus of the coating 2 is a single variable, the surface compressive stress ( $\sigma_{c1} + \sigma_{c2}$ ) increases with the increase of  $E_{c2}/E_s$ ; according to Figure 4, when the shrinkage rate of the coating 2 is a single variable, the surface compressive stress ( $\sigma_{c1} + \sigma_{c2}$ ) decreases with the increase of  $\alpha_{c2}/\alpha_s$ ; Figures 3 and 4 show that the surface compressive stress ( $\sigma_{c1} + \sigma_{c2}$ ) increases first with the increase of  $S_s/S_c$ , and plateaus after  $S_s/S_c > 80$ . Similarly, when the elastic modulus value of the coating 2 is taken as invariants, and the shrinkage rate value and the elastic modulus value of the coating 1 are the variables, the trend of surface compressive stress changes with the cross-sectional area ratio value of the substrate and the coating, which is completely consistent with the above.

Considering the above analysis: (1) on the premise of coating 2 shrinkage < coating 1 shrinkage < substrate shrinkage, the smaller the shrinkage of coating 1 and coating 2, the greater the surface compressive stress. (2) The higher the elastic modulus of coating 1 and coating 2, the greater the surface compressive stress. (3) In order to obtain enough surface compressive stress, it is suggested that  $S_s/S_c > 80$ .

### 3. Experiment

**3.1. Materials.** According to the above theoretical analysis, it can be seen that the shrinkage rate of coating 2 < that of coating 1 < that of substrate is the prerequisite for the generation of surface compressive stress, and the concrete will contract during the hardening process. Therefore, in this study, the slightly expanded sulphoaluminate cement was selected as the main component of the coating material, and the shrinkage rate of the coating material was adjusted by adding different amounts of concrete efficient expansion agent, so as to ensure the smooth generation of surface compressive stress.

Ordinary Portland cement (P·O42.5R) and sulphate aluminate cement (SAC42.5) were selected as cement in the concrete substrate and coating, respectively. Fine aggregate in substrate was medium sand with fineness modulus  $M_x$



FIGURE 7: Flexural strength test.



FIGURE 8: Elastic modulus test of coating.

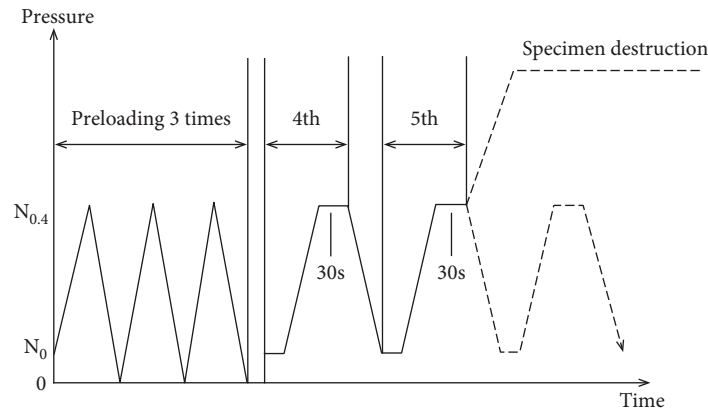


FIGURE 9: Schematic diagram of the loading method of the coating elastic modulus.

$= 2.82$ , and the coarse aggregate was stone with continuous gradation of 5~30 mm in particle size. Calcium oxide-calcium thialuminite compound expansion agent (HME®-IV) was used for the expansion agent, and water was laboratory tap water. The chemical composition of the cement and the expansion agent is shown in Table 1, and the performance indicators of the expansion agent are shown in Table 2.

**3.2. Design of Coating and Substrate.** In order to facilitate the test of the shrinkage rate and elastic modulus of the coating material, the low content of expansion agent and sulphate aluminate cement was selected as the coating in this experiment, and five groups of test schemes were designed. Among them, the blank test group without coating had a total of one group; the single-layer coating consisted of three groups, which were composed of sulphate aluminate cement and 0%, 6%, and 10% expansion agent, respectively. There was a group of double-layer gradient coating, the first layer and the second layer were the substrate of sulphate aluminate cement and expansion agent with the contents of 0% and 10%, respectively, so that the shrinkage difference between the two layers reaches the maximum. The water-cement ratio of the coating is 0.5, and the mixture ratio of the reference specimen without the coating and the substrate with the coating were consistent. The mixture ratio of the coating and the substrate is given in Table 3.

### 3.3. Methods

**3.3.1. Preparation of Coated Concrete Test Specimens.** After the concrete substrate was poured, solid, and flattened, it shall be covered with plastic film and placed in the room with an ambient temperature of  $(20 \pm 1)^{\circ}\text{C}$ . After 24 h, the concrete surface shall be cleaned and moistened with a wet rag. The prepared coating was evenly sprayed on the concrete surface (four faces in the length direction) and smoothed with a scraper. Double-layer gradient coating sprays the second coating immediately after spraying the first coating and smoothing with a scraper, and the test schematic diagram is shown in Figure 5, where  $k$  is a cross-section,  $h_1$  for the thickness of the first coating, and  $h_2$  for the



FIGURE 10: Elastic modulus test of substrate.

thickness of the second coating. The specific preparation process of coated concrete specimen is shown in Figure 6.

**3.3.2. Flexural Strength Test.** The prepared specimens were cured to 7d and 28d at  $(60 \pm 5)\%$  relative humidity and  $(20 \pm 1)^{\circ}\text{C}$ , and then, according to GB/T 50081-2019 guidelines, the specimens of size  $100\text{ mm} \times 100\text{ mm} \times 400\text{ mm}$  were tested for measuring flexural strength by universal testing machine (Figure 7), and the controlled loading rate was 0.05 MPa/s. Take the average value of the flexural strength test results of a group of 3 specimens as the test result.

**3.3.3. Coating and Substrate Shrinkage Rate Test.** According to JC/T 313-2009 guidelines, the specimen size of  $25\text{ mm} \times 25\text{ mm} \times 280\text{ mm}$  was tested for measuring shrinkage rate of the coating by JH-320 alkali aggregate specific length meter. Specimen size of  $100\text{ mm} \times 100\text{ mm} \times 515\text{ mm}$  was tested for measuring shrinkage rate of the concrete by HSP-540 shrinkage apparatus as per GB/T 50082-2009 guidelines. After the molding of the specimen, the initial length was measured after the curing condition of 1d under the above discount strength test, the specimen length changes after curing to 28d to calculate the shrinkage rate of 28d age, and the shrinkage rate of the coating and

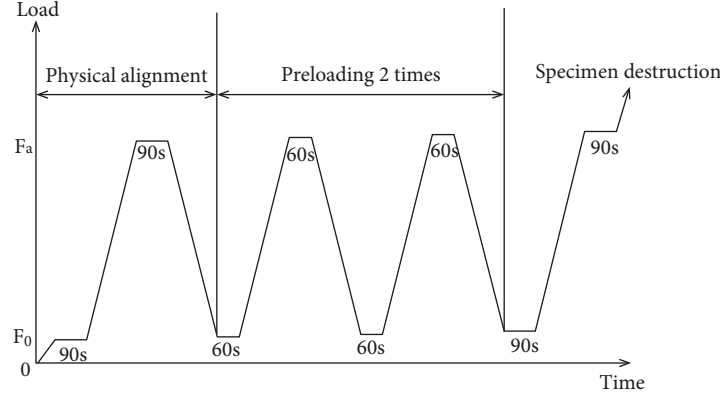


FIGURE 11: Schematic diagram of the loading method of the substrate elastic modulus.

TABLE 4: Test results of shrinkage rate and elastic modulus of coating and concrete.

Sample no.	$S_s/\text{mm}^2$	$S_c/\text{mm}^2$	$\alpha_s/\%$	$\alpha_c/\%$	$E_s/\text{MPa}$	$E_c/\text{MPa}$
SC-0%	10000	100	-0.330	0.020	$2.81 \times 10^4$	$1.80 \times 10^4$
SC-6%	10000	100	-0.330	0.056	$2.81 \times 10^4$	$2.00 \times 10^4$
SC-10%	10000	100	-0.330	0.081	$2.81 \times 10^4$	$1.75 \times 10^4$
Sample no.	$S_s/\text{mm}^2$	$S_c/\text{mm}^2$	$\alpha_s/\%$	$\alpha_{c1} \alpha_{c2}/\%$	$E_s/\text{MPa}$	$E_{c1} E_{c2}/\text{MPa}$
DC-0%-10%	10000	100	-0.330	0.020 0.081	$2.83 \times 10^4$	18000 17500

substrate was calculated as the formula:

$$S_{28} = \frac{(L_{28} - L_1)}{L_0} \times 100\%. \quad (16)$$

In formula,  $S_{28}$  indicates the shrinkage rate of 28d (positive expansion and negative contraction);  $L_{28}$  is the length of 28d, mm;  $L_1$  is the initial length of the specimen, mm;  $L_0$  is the effective length of the specimen (coating specimen 250, substrate specimen 485), mm. Take the average value of the shrinkage rate test results of a group of 3 specimens as the test result.

**3.3.4. Coating and Substrate Elastic Modulus Test.** In order to calculate the theoretical value of surface residual compressive stress generated in the coating, the elastic modulus of the coating and the concrete substrate at the age of 28d were tested by the dial indicator method. Specimen size of 70.7 mm × 70.7 mm × 220 mm was tested for measuring elastic modulus of the coating by TM-3 mortar elastic modulus tester as per JGJ/T70-2009 guidelines (Figure 8), and the loading speed was set to 0.5kN/s. The schematic diagram of the loading method is shown in Figure 9,  $N_0$  is the initial load at a stress of 0.3 MPa and  $N_{0.4}$  is the pressure at 40% of the axial compressive strength.

Specimen size of 150 mm × 150 mm × 300 mm was tested for measuring elastic modulus of the concrete substrate by TM-2 concrete elastic modulus tester as per GB/T 50081-2019 guidelines (Figure 10), and the loading speed was set to 0.3 MPa/s. The schematic diagram of the loading method is shown in Figure 11,  $F_0$  is the initial load with a stress of 0.5 MPa, and  $F_a$  is the load at 1/3 axial compressive

strength. Take the average value of the elastic modulus test results of a group of 3 specimens as the test result.

**3.3.5. Microscopic Test.** The interface morphology and microstructure between coating and substrate were observed by JSM-6360LV scanning electron microscope. The sample preparation steps were as follows: after the flexural strength test of the specimen, a small sample was cut at the section of the specimen to be tested and then immersed in anhydrous ethanol solution for 24 h to stop the hydration reaction; finally, the test sample was placed in a 100°C oven for drying for 12 h. The surface of the sample to be tested needs to be sprayed with gold for 30 min before using scanning electron microscope to observe the sample, so as to increase the conductivity of the sample and make the observation of the interface microstructure clearer.

## 4. Results and Discussion

**4.1. Theoretical Value Calculation of Surface Compressive Stress.** According to the qualitative analysis in Section 2, the thickness of the coating should be less than 1.25 mm. Therefore, the thickness  $h$  of the single-layer coating and the thickness  $h_1$  and  $h_2$  of the double-layer gradient coating were both set to 1 mm in the test of this study, that was, the cross-sectional area ratio of coating to substrate remained unchanged. In order to verify that the surface compressive stress of the gradient coating is greater than that of the change of coating shrinkage rate and elastic modulus, the shrinkage rate and elastic modulus were tested (Table 4), and the theoretical values of the surface compressive stress



TABLE 5: Theoretical values of the surface compressive stress in the coating.

Sample no.	$S_s/S_c$	$E_s/E_c$	$\alpha_c / \alpha_s$	$E_s/\text{MPa}$	$ \alpha_s /\%$	$\sigma_c/\text{MPa}$
SC-0%	100	1.56	-0.61	$2.81 \times 10^4$	0.330	9.48
SC-6%	100	1.41	-1.70	$2.81 \times 10^4$	0.330	17.67
SC-10%	100	1.61	-2.45	$2.81 \times 10^4$	0.330	19.83
Sample no.	$S_s/S_c$	$E_{c1}/E_s E_{c2}/E_s$	$\alpha_{c1} / \alpha_s \alpha_{c2}/\alpha_s$	$E_s/\text{MPa}$	$ \alpha_s /\%$	$\sigma_{c1} + \sigma_{c2}/\text{MPa}$
DC-0%-10%	100	0.64 0.62	-0.61 -2.45	$2.83 \times 10^4$	0.330	29.02

Note: When the surface compressive stress is calculated, the shrinkage of the substrate is absolute value.

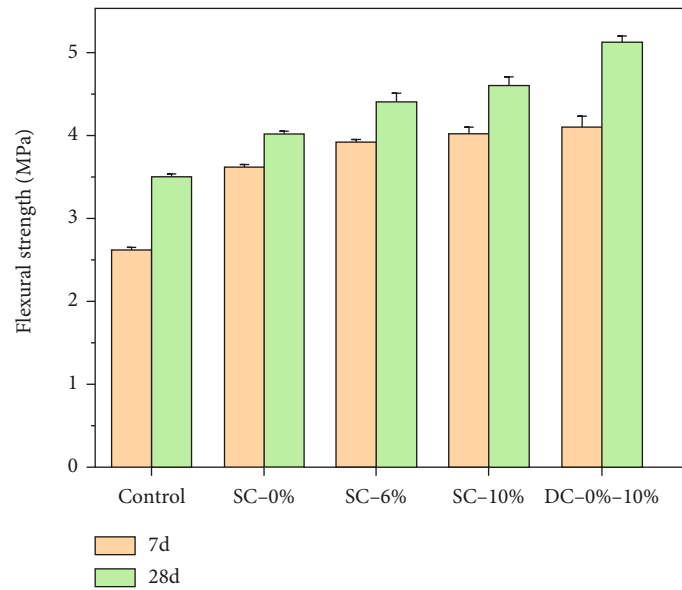


FIGURE 12: Flexural strength of uncoated specimens and coated specimens.

were calculated based on Equations (14) and (15), respectively. The calculation results are shown in Table 5.

According to Table 4, the shrinkage rate of all coating materials is positive and still expanding at 28d, while the concrete substrate is shrinking, and the shrinkage rate is coating 2 < coating 1 shrinkage rate, which shows that the coatings used in the test meet the prerequisite conditions for generating surface compressive stress.

The SC-0% group is the single-layer coating group without expansion agent in the coating, and the DC-0%-10% group is the double-layer gradient coating group with 10% expansion agent content on the basis of SC-0% group. It can be seen from Table 5, the surface compressive stress in the coating of DC-0%-10% group is 29.02 MPa, the surface compressive stress is increased by 206.1% compared with the SC-0% group. The coating of SC-10% in the single-layer coating group was the same as that of coating 2 in the double-layer gradient coating group, and the surface compressive stress in the coating of DC-0%-10% group was still higher than that of SC-10% group by 9.19 MPa. In the three single-layer coating groups, with the increase of the content of expansion agent in the coating from 0% to 10%, the shrinkage rate of the coating showed a downward

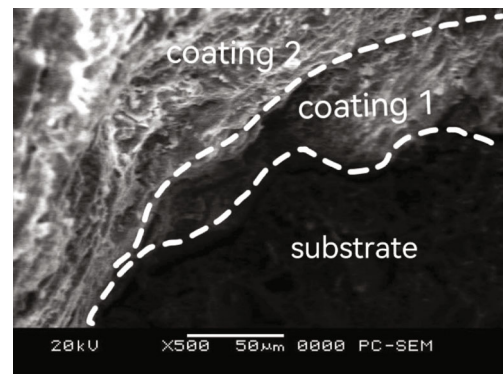


FIGURE 13: Interface morphology between coating and substrate.

trend, while the elastic modulus of the coating changed little, and the surface compressive stress in the coating increased.

The above analysis shows the following. (1) The surface compressive stress generated by the double-layer gradient coating group is significantly higher than that generated by the single-layer coating group, which also verifies the conclusion of the theoretical derivation of the double surface

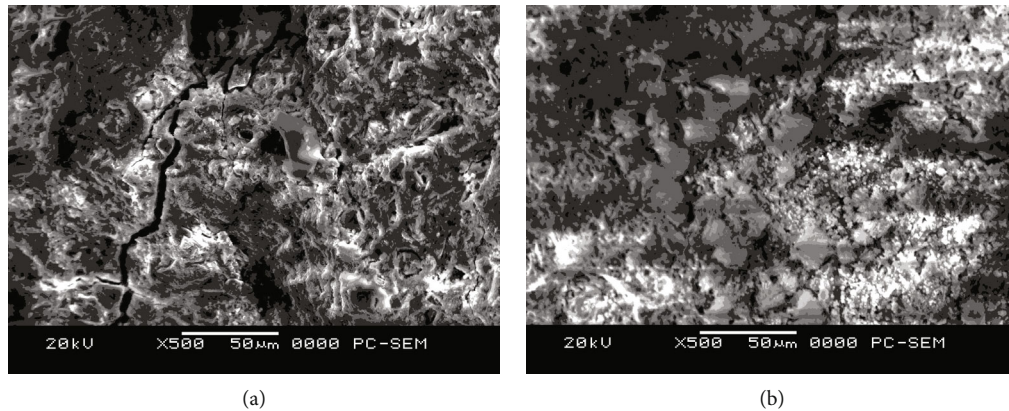


FIGURE 14: Internal morphology of substrate at interface between uncoated specimen (a) and coated specimen (b).

compressive stress in Section 2. (2) When the cross-sectional area ratio of the coating to the substrate is a fixed value and the elastic modulus ratio changes little, with the decrease of the coating shrinkage, the surface compressive stress in the coating increases, which is consistent with the conclusion obtained in the qualitative analysis.

**4.2. Experimental Verification of Improving Flexural Strength of Concrete.** To further verify the improvement effect of the double-layer gradient coating on the flexural strength of concrete than the single-layer coating and to study the influence of the surface compressive stress on the flexural strength of concrete, the 7d and 28d flexural strength of uncoated and coated specimens were tested. The test results are shown in Figure 12.

It can be seen from Figure 12 that compared with the reference specimen without coating, whether single-layer coating or double-layer gradient coating can improve the 7d and 28d flexural strength of concrete, even the lowest group of 7d flexural strength in the coated specimen (SC-0%) also reached the 28d flexural strength of the reference specimen without coating (Control).

The effect of surface compressive stress on the early flexural strength of concrete was better than that on the later flexural strength. In the single-layer coating group, 7d and 28d flexural strength of concrete specimens increases with the increase of expansion agent content in the coating. The 7d and 28d flexural strength improvement rates of SC-0% group were 38.5% and 14.3%, respectively, the improvement rates of 7d and 28d flexural strength in SC-6% group were 50.0% and 25.7%, respectively, and the 7d and 28d flexural strength improvement rates of SC-10% group were 53.8% and 31.4%, respectively. The flexural strength of double-layer gradient coating group (DC-0%-10%) was better than that of the other three single-layer coating groups. The early and late flexural strength was 4.1 MPa and 5.1 MPa, respectively, and the strength improvement rate was 57.7% and 45.7%. This shows that the method proposed in this study to produce double surface compressive stress by coating double-layer gradient coating on the surface of concrete is feasible and effective for improving the flexural strength at early and late stages.

Combined with the theoretical values of surface compressive stress in Section 4.1 and the test results of flexural strength in this section, it can be found that the compressive stress on the surface of concrete and the improvement effect on the flexural strength of concrete with coated double-layer gradient coating are greater than those with coated single-layer coating. In the single-layer coating group, under the premise of small changes in the elastic modulus of the coating, with the increase of the content of expansion agent in the coating, the shrinkage rate of the coating decreases, and the surface compressive stress generated in the coating increases. The improvement effect on the flexural strength of concrete is also becoming more and more obvious. It can be seen that the greater the surface compressive stress generated in the coating, the better the effect of improving the flexural strength of concrete.

**4.3. SEM Microanalysis.** Good adhesion between the coating and the concrete substrate is the premise of the surface residual compressive stress, and it is also the key to the overall and common stress of the concrete components after coating. Figure 13 shows the micromorphology of the interface between the double-layer coating and the concrete substrate at the age of 28d. It can be observed from the figure that the boundary between the coating and the substrate is obvious and closely integrated, indicating that the cement slurry with expansion agent as the coating can better bond with the concrete substrate and further generate surface residual compressive stress.

Figure 14 shows the SEM comparison results of the concrete substrate at the interface between the double-layer gradient coating and the uncoated specimen at the age of 28d. Figure 14(a) shows that there are obvious cracks in the substrate of uncoated concrete, and the overall structure is uneven and irregular; compared with the uncoated specimen, the overall structure of the double-layer coated concrete substrate in Figure 14(b) is dense, and the internal cracks are significantly reduced.

This phenomenon may be due to the coating increases the wettability of the substrate surface and improves the water-cement ratio between the coating and the substrate, which promotes the hydration of the interface cement. At

the same time, the expansion agent reacts to generate a large number of Aft crystals that are interwoven to fill and cut off the capillary pores, so that the large pores are reduced and the total porosity is reduced, thereby improving the compactness of the microstructure at the interface [34]. The improvement of the pore structure at the interface by the coating reduces the overall moisture loss of the specimen, thereby reducing the shrinkage stress caused by the moisture loss of the pores, which is conducive to reducing the shrinkage cracking of concrete. In addition, the in-plane compressive stress of the surface itself is compressed and densified, which hinders the expansion of surface microcracks, and can improve the flexural strength of concrete [2].

The above microscopic analysis results show that the improvement effect of low shrinkage coating on the flexural strength of concrete is due to the fact that the generated surface compressive stress reduces the tensile stress caused by the external load and inhibits the generation and propagation of surface cracks. On the other hand, it is due to the improvement effect of coating on the structure of the interfacial transition zone.

## 5. Conclusions

- (1) The theoretical analysis of double-layer gradient coating enhancing concrete flexural strength shows that the size of the surface compressive stress is related to the cross-section product ratio, elastic modulus ratio, and shrinkage rate ratio of the substrate and the coating, so through these parameters, the size of the surface compressive stress can be adjusted to achieve the optimal design effect. When the parameters of the substrate are unchanged, the higher the elastic modulus of the coating, the greater the surface compressive stress; the smaller the shrinkage of the coating, the greater the surface compressive stress; when the cross-sectional area ratio of substrate to coating is more than 80, the surface compressive stress is larger
- (2) Coated on the concrete surface by double-layer gradient coating, the first layer is pure sulfate cement mixed with 10% expansion agent, Because the shrinkage rate of Coating 1 is between that of concrete and Coating 2, surface compressive stresses are formed between Coating 1 and Coating 2, and between Coating 1 and concrete, respectively, during the curing process. which effectively improves the early and later fracture strength by 77.7% and 45.7%, respectively, compared with the uncoated reference test
- (3) By combining the theoretical value of surface compressive stress of the coating test and the flexural strength test results, it was found that the double-layer gradient coating test produces more surface compressive stress and higher flexural strength than the single-layer coating test; the smaller the shrinkage rate of the coating, the greater the surface com-

pressive stress, the higher the flexural strength. It can be shown that the greater the surface compressive stress generated in the coating, the better the improvement effect of the concrete flexural strength

- (4) SEM test results show that the coating mixed with expansion agent and cement can be safely and stably attached to the concrete substrate. The coating can improve the density of the interface with the substrate and hinder the formation and propagation of surface cracks

The strengthening method adopted in this study can provide a new idea for improving the flexural strength of cement-based materials, but there are still some problems that need further study, mainly including the following:

- (1) The more specific relationship between the ratio of different cross-sectional area, elastic modulus ratio and shrinkage ratio, and the flexural strength of specimens is taken as the focus of future research
- (2) In the future research, various types of coatings can be selected for further study to further increase the effect of surface residual compressive stress on the flexural strength of concrete
- (3) In the future research, the coating can be coated by machine, which can reduce the deviation of the test results caused by manual operation

## Data Availability

Data sharing is not applicable to this article as no new data were created or analyzed in this study.

## Conflicts of Interest

The authors declare that they have no conflicts of interest.

## Acknowledgments

This work was supported by the National Natural Science Foundation of China (Grant No. 52032011), the Education Department Foundation of Liaoning Province (Grant No. LJKZ1177), and the Department of Science & Technology Guidance Plan Foundation of Liaoning Province (Grant No. 2019JH8/10100091).

## References

- [1] L. H. Zhang, M. H. Tan, Y. P. Ma, and K. R. Wu, "Study on properties of bonding and shrinkage cracking of PP fiber cement [J]," *Building Materials Journal*, vol. 1, pp. 17–21, 2001.
- [2] J. S. Qian, D. Qiao, L. Shi, Y. D. Dang, and Z. Wang, "Influence of external coating on concrete properties and mechanism of action [J]," *Journal of the Chinese Ceramic Society*, vol. 37, no. 12, pp. 2090–2096, 2009.
- [3] C. J. Shi, A. Jiménez, A. F. Palomo, and A. Palomo, "New cements for the 21st century: the pursuit of an alternative to

- Portland cement [J],” *Cement and Concrete Research*, vol. 41, no. 7, pp. 750–763, 2011.
- [4] S. Tolmachov, O. Belichenko, D. Zakharov, G. Vatulia, A. Plugin, and O. Darenskyi, “Influence of additives on flexural strength of concrete,” *MATEC Web of Conferences*, vol. 116, article 01019, 2017.
  - [5] S. Singh, G. D. Ransinchung, and P. Kumar, “Effect of mineral admixtures on fresh, mechanical and durability properties of RAP inclusive concrete,” *Construction and Building Materials*, vol. 156, pp. 19–27, 2017.
  - [6] M. M. Zhang, S. L. Wang, S. M. Zhang, and B. Zhang, “Effect of mineral admixtures on mechanical properties of recycled concrete [J],” *Bulletin of the Chinese Ceramic Society*, vol. 36, no. 5, pp. 1505–1511, 2017.
  - [7] S. H. M. Adanagouda and H. M. Somasekharaiah, “Strength and durability studies on hybrid fiber reinforced high-performance concrete for silica fume based mineral admixture,” *IOP Conference Series: Earth and Environmental Science*, vol. 822, no. 1, article 012041, p. 012041, 2021.
  - [8] S. A. Mahadik, S. K. Kamane, and A. C. Lande, “Effect of steel fibers on compressive and flexural strength of concrete [J],” *International Journal of Advanced Structures and Geotechnical Engineering*, vol. 3, no. 4, pp. 388–392, 2014.
  - [9] A. A. Bhat and S. Alam, “Impact of steel fiber on the mechanical property of concrete containing mineral admixture,” *IOP Conference Series: Earth and Environmental Science*, vol. 889, no. 1, article 012004, 2021(8pp).
  - [10] J. Bi, Y. C. Zhang, W. W. Chen, W. Liu, and L. Y. Xiong, “Study on the effect of polypropylene fiber on mechanical performance of concrete [J],” *Bulletin of the Chinese Ceramic Society*, vol. 34, no. 6, pp. 1694–1699, 2015.
  - [11] V. Turlapati and V. Chintapalli, “A comparative study on performance of synthetic and natural fibers on compressive and flexural strength of concrete,” *Advanced Engineering Forum*, vol. 36, pp. 97–113, 2020.
  - [12] M. Wyrzykowski, G. Terrasi, and P. Lura, “Expansive high-performance concrete for chemical-prestress applications,” *Cement and Concrete Research*, vol. 107, pp. 275–283, 2018.
  - [13] Y. L. Yang, Q. Y. Ma, H. Q. Fei, Y. Y. Zhang, and J. S. Zhang, “Test and analysis of the influence of moisture content and expansion agent on the fold resistance of ready-mixed compensation shrinkage concrete [J],” *Concrete*, vol. 2, pp. 128–131, 2015.
  - [14] R. Li, D. Z. Wang, and Y. F. Meng, “Study on mechanical properties of fly ash ceramsite concrete reinforced by mineral admixtures [J],” *Bulletin of Science and Technology*, vol. 32, no. 2, pp. 92–95+99, 2016.
  - [15] M. Saafi, L. Tang, J. Fung, M. Rahman, and J. Ligat, “Enhanced properties of graphene/fly ash geopolymeric composite cement,” *Cement and Concrete Research*, vol. 67, pp. 292–299, 2015.
  - [16] Z. K. Wang, J. Fan, and G. Y. Li, “Effect of carbon nanotubes/polyvinyl alcohol on mechanical properties and drying shrinkage of concrete [J],” *Journal of the Chinese Ceramic Society*, vol. 48, no. 10, pp. 1653–1658, 2020.
  - [17] Q. Liu, Z. Lu, X. Liang, R. Liang, Z. Li, and G. Sun, “High flexural strength and durability of concrete reinforced by *in situ* polymerization of acrylic acid and 1-acrylamido-2-methylpropanesulfonic acid,” *Construction and Building Materials*, vol. 292, p. 123428, 2021.
  - [18] Y. M. Chen, X. Y. He, Y. X. Li, and Y. Su, “Research progress and existing problems of mineral admixtures [J],” *Materials Reports*, vol. 8, pp. 28–31, 2006.
  - [19] G. A. Rao, “Long-term drying shrinkage of mortar – influence of silica fume and size of fine aggregate,” *Cement and Concrete Research*, vol. 31, no. 2, pp. 171–175, 2001.
  - [20] M. S. Meddah, M. A. Ismail, S. El-Gamal, and H. Fitriani, “Performances evaluation of binary concrete designed with silica fume and metakaolin,” *Construction and Building Materials*, vol. 166, pp. 400–412, 2018.
  - [21] S. A. Kagadgar, S. Saha, and C. Rajasekaran, “Mechanical and durability properties of fly ash based concrete exposed to marine environment,” *Selected Scientific Papers—Journal of Civil Engineering*, vol. 12, no. 1, pp. 7–18, 2017.
  - [22] Y. Shi, J. H. Zhu, D. L. He, X. D. Luo, and T. Wu, “Effect of mineral admixtures on mechanical properties and cracking trend of concrete [J],” *Journal of the Chinese Ceramic Society*, vol. 47, no. 11, pp. 1605–1610, 2019.
  - [23] M. Bai, D. T. Niu, L. Jiang, and Y. Y. Miao, “Study on improving mechanical properties and microstructure of concrete with steel fiber [J],” *Bulletin of the Chinese Ceramic Society*, vol. 32, no. 10, pp. 2084–2089, 2013.
  - [24] F. Yi, “Research progress of plant fiber concrete [J],” *Construction Materials & Decoration*, vol. 34, pp. 125–126, 2017.
  - [25] J. X. Wang and L. J. Wang, “Research progress on the application of nanomaterials in concrete [J],” *Concrete*, vol. 11, pp. 18–21, 2004.
  - [26] Z. Y. Xie, H. Zhou, Q. C. Li, and D. X. Li, “Research progress in preparation of nano-silica sol and its application in cement-based materials [J],” *Materials Reports*, vol. 34, no. S2, pp. 1160–1163, 2020.
  - [27] P. M. Wang, G. R. Zhao, and G. F. Zhang, “Mechanism of redispersible emulsion powder in cement mortar [J],” *Journal of the Chinese Ceramic Society*, vol. 46, no. 2, pp. 256–262, 2018.
  - [28] K. Li, Z. Q. Wei, H. X. Qiao, C. G. Lu, and J. Guo, “Research progress on the effect of four kinds of admixtures on the properties of polymer modified cement-based materials [J],” *Materials Reports*, vol. 35, no. S1, pp. 654–661, 2021.
  - [29] D. J. Green, R. Tandon, and V. M. Sglavo, “Crack arrest and multiple cracking in glass through the use of designed residual stress profiles,” *Science*, vol. 283, no. 5406, pp. 1295–1297, 1999.
  - [30] L. Wondraczek, J. C. Mauro, J. Eckert et al., “Towards ultra-strong glasses,” *Advanced Materials*, vol. 23, no. 39, pp. 4578–4586, 2011.
  - [31] J. C. Mauro, C. S. Philip, D. J. Vaughn, and M. S. Pambianchi, “Glass science in the United States: current status and future directions,” *International Journal of Applied Glass Science*, vol. 5, no. 1, pp. 2–15, 2014.
  - [32] Y. W. Bao, F. H. Kuang, Y. Sun et al., “A simple way to make pre-stressed ceramics with high strength,” *Journal of Materials*, vol. 5, no. 4, pp. 657–662, 2019.
  - [33] Y. W. Bao, Y. Sun, F. H. Kuang, F. H. Li, and D. T. Wan, “The development and exploration of high-strength prestressed ceramics [J],” *Journal of Inorganic Materials*, vol. 35, no. 4, pp. 399–406, 2020.
  - [34] L. Huang, W. D. Zhuo, Y. Gu, G. P. Shang, and X. Y. Huang, “Experimental study on influence of interface agent on interface bonding performance of new and old concrete [J],” *Journal of Fuzhou University (Natural Science Edition)*, vol. 46, no. 3, pp. 396–402, 2018.